Revue des Energies Renouvelables Vol. 18 N°4 (2015) 633 – 641

Numerical study of mixed convection flows in a U-shaped channel

M. Naoum* and M. El Alami

Laboratoire de Physique des Matériaux, Microélectronique, Automatique et Thermique
Faculté des Sciences Aïn Chock, Université Hassan II,
8 km, Route d'El Jadida, B.P. 5366, Maarif, Casablanca 20100, Maroc

(reçu le 10 Novembre 2015 – accepté le 7 Décembre 2015)

Abstract - *In this work, we study numerically mixed convection flows in an open U-shaped channel. The right opening lets pass fresh air at cold temperature TC, while the walls of the channel are heated at the temperature TH > TC. Our study is based on a volume control method performed for 100 < Re < 700, Ra = 10^5 and Pr = 0.72. Results are presented in terms of thermal and dynamic fields, Nusselt number variation with Re, flow velocities and temperatures at the channel outlet.*

Résumé – *Dans ce travail, nous étudions les flux de convection numériquement mixtes dans un canal ouvert en forme de U. L'ouverture à droite laisse entrer l'air frais dans des températures fraîches T_C, tandis que les parois du canal sont chauffées à une température $T_H > T_C$. Notre étude est basée sur la méthode du volume contrôlé pour les valeurs 100<Re<700, Ra=10^5 et Pr=0.72. Les résultats sont présentés pour les domaines thermiques et dynamiques, la variation du nombre de Nusselt avec le Re, la vitesse de l'écoulement et les températures à la sortie du canal.*

Keywords: U-shaped channel - Mixed convection - Numerical study - Air-ground exchanger - Canadian well.

1. INTRODUCTION

The study of convection flows in an open U-shaped channel has a practical interest in different areas, such as the pre-air conditioning system for its cooling, which is called the Canadian well.

This air-ground heat exchanger has often been the subject of several experimental and numerical studies in recent years. It has enabled to establish reliable rules and design tools for different configurations [1, 2]. Improvements in geometry also allowed optimizing energy performance.

Many works have been made in this subject. In particular, we can include the work of Dehina [3] who proposed a numerical simulation of a heat exchanger air - ground to improve energy efficiency; he incorporated a coaxial tube having a low section carrying irrigation's water at a constant temperature.

Naili *et al.*, [4] studied the opportunity to use the thermal inertia for heating soil: an analytical study validated by experimental results, allowed them to assess the thermal performances and optimize the operating parameters of the exchanger.

Mebarki *et al.*, [5] studied the air conditioning by Canadian well in arid areas. They studied the influence of the geometrical parameters on the temperature inside the exchanger. They found that the dry soil is more inert and more efficient in term of heat exchange. They finalized their study by varying the geometrical parameters and they prove that the optimum length value is 25 m with constant depth equal to 3 m, to achieve the soil temperature (20 °C) for the comfort air conditioning.

* naoum.meryem8910@gmail.com

In this work, we study the mixed convection air flows in an open U-shaped channel representing a Canadian well. The originality of our study is the introduction of several control parameters affecting the flow and heat transfer in the channel. On the other hand the different types of boundary conditions that we will discuss later in this work will value more our approach. In this paper, we present the first results of the influence of some parameters on the temperature and average velocity at the channel outlet and on the global Nusselt number.

2. STUDIED CONFIGURATION AND MATHEMATIC FORMULATION

The studied configuration is shown in Figure 1. This is an open U-form channel ventilated by cold air in the inlet (right opening) at the temperature (T_C, $\theta = 0$), the channel walls are maintained at a hot temperature ($T_H > T_C$, $\theta_H = 1$).

We assume that the flow and heat transfer are two-dimensional and the physical properties of air are constant and the Boussinesq approximation is validated.

$$\frac{\partial^2 V}{\partial Y^2} = 0, \frac{\partial^2 \theta}{\partial Y^2} = 0, U = 0 \qquad \theta_C = 0, U = 0, V = -1$$

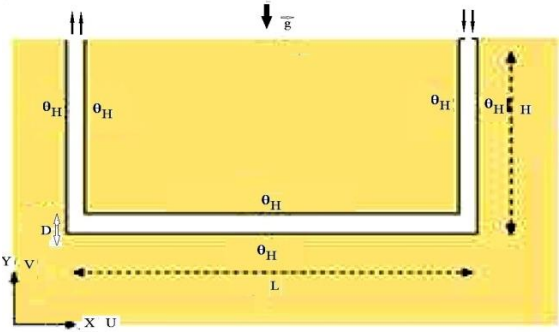

Fig. 1: Studied configuration

Referring to figure 1, the dimensionless variables are defined as follows:

$$l = \frac{L}{D}, \; h = \frac{H}{D}, \; \tau = \frac{t}{D / V_0}, \; U = \frac{u}{V_0},$$

$$V = \frac{v}{V_0}, \; P = \frac{P}{\rho V_0^2}, \theta = \frac{T - T_f}{T_C - T_f}$$

With, D, Characteristic channel diameter, V_0, Characteristic velocity, D / V_0, Characteristic time, ρV_0^2, Characteristic pressure.

The dimensionless transient equations in terms of temperature θ, driving pressure P and velocity U and V are written in the form:

■Mass conservation equation

$$\frac{\partial U}{\partial X} + \frac{\partial V}{\partial Y} = 0 \qquad (1)$$

■Momentum conservation equation

According to X

$$\frac{\partial U}{\partial \tau} + U\frac{\partial U}{\partial X} + V\frac{\partial U}{\partial Y} = -\frac{\partial P}{\partial X} + \frac{1}{Re}\left(\frac{\partial^2 U}{\partial X^2} + \frac{\partial^2 U}{\partial Y^2}\right) \tag{2}$$

According to Y

$$\frac{\partial U}{\partial \tau} + U\frac{\partial V}{\partial X} + V\frac{\partial V}{\partial Y} = -\frac{\partial P}{\partial Y} + \frac{1}{Re}\left(\frac{\partial^2 V}{\partial X^2} + \frac{\partial^2 V}{\partial Y^2}\right) + \frac{Gr}{Re^2}\theta \tag{3}$$

■Energy conservation equation

$$\frac{\partial \theta}{\partial \tau} + U\frac{\partial \theta}{\partial X} + V\frac{\partial \theta}{\partial Y} = +\frac{1}{RePr}\left(\frac{\partial^2 \theta}{\partial X^2} + \frac{\partial^2 \theta}{\partial Y^2}\right) \tag{4}$$

The boundary conditions associated to these equations are defined as:

-At the inlet of the channel- $\theta = \theta_C = 0$, $V = V_{in} = -1$, $U = 0$

-At the outlet of the channel- $U = 0$, $\frac{\partial^2 \theta}{\partial Y^2} = 0$, $\frac{\partial^2 V}{\partial Y^2} = 0$

-On the channel walls- $U = V = 0$, $\theta = \theta_H = 1$

-**Nusselt number**

The mean Nusselt number is calculated along the hot walls of the channel using this equation:

$$\begin{aligned} Nu = &\int_0^H \frac{\partial T}{\partial x}\Big]_{x=0} dy + \int_D^H \frac{\partial T}{\partial x}\Big]_{x=D} dy + \int_0^L \frac{\partial T}{\partial y}\Big]_{x=0} dx \\ &+ \int_D^{L-D} \frac{\partial T}{\partial y}\Big]_{x=0} dx + \int_0^H \frac{\partial T}{\partial x}\Big]_{x=L} dy + \int_D^H \frac{\partial T}{\partial x}\Big]_{x=L-D} dy \end{aligned} \tag{5}$$

3. NUMERICAL METHOD

The results presented in this work, have been obtained by using numerical procedure based on a finite volume technique [8]. The governing equations were solved considering the Boussinesq approximation. Two dimensional flows are considered in this study and the velocity – pressure coupling is solved by using Simplec algorithm [9].

As a result of a grid independence study, a grid size of 80 × 160 was found to model accurately the flow fields described in this work. Time steps considered are ranging between 10^{-4} and 10^{-3}.

The accuracy of the numerical model was verified by comparing our results with those obtained by De Val Devis *et al.* [10] and Le Queré *et al.* [11] for natural convection in differential heated cavity, **Table 1**, and then with the results obtained by Kalache *et al.* [12] in a trapezoidal cavity, **Table 2**.

Finally, we have confronted our results to those proposed by Desrayaud *et al.* [13] in a vertical channel with two ribs symmetrically placed on the channel walls, **Table 3**. Good agreement was obtained in Ψ_{max} and Nu_m terms.

Table 1: Comparison of our results and those of De Val Devis *et al.* [10], Le Queré *et al.* [11]

Ra	De Val Devis *et al.* [10]	Le Queré *et al.* [11]	Present study	Maximum deviation
10^4	Ψ_{max} =5.098	---	Ψ_{max} =5.035	1.2%
10^5	Ψ_{max} =9.667	---	Ψ_{max} =9.725	0.6%
10^6	Ψ_{max} =5.098	16.8110	Ψ_{max} =17.152	0.2%
10^7	---	30.170	Ψ_{max} =30.077	0.3%

Table 2: Comparison of our results with those of Kalache *et al.* [12]

Gr	Present study	Kalache *et al.* [12]	Maximum deviation
2.5×10^3	Ψ_{max} =5.42	Ψ_{max} =5.37	2.4%
5×10^3	Ψ_{max} =9.74	Ψ_{max} =9.77	3%
10^4	Ψ_{max} =15.43	Ψ_{max} =15.41	0.2%

Table 3: Comparison of our results with those of Desrayaud *et al.* [13]

Ra=10^5 (A=5)	Desrayaud et al. [13]	Present study	Maximum deviation
Ψ_{max}	151.51	152.85	0.9%
Nu_m	148.27	151.72	2.2%

4. RESULTS AND DISCUSSION

In this paper, the analysis is focused on heat transfer rate across the hot walls, flow and thermal fields for Rayleigh number: $Ra = 10^5$, Reynolds number: $100 \le Re \le 700$ and other parameters of the problem (l =2m, d =0.2m, h =1m and $Pr = 0.72$). Rayleigh number values and Reynolds number ranges are chosen in favor of mixed convection role.

The particularity of this problem is the appearance of different solutions when varying Reynolds number. The flow structure is, essentially, composed of the open lines, which represent the forced flow, and closed cells which are due to the recirculation movement up of the jet or to natural convection phenomena. In this later case, the cells are dawn of the forced flow, localized substantially in the right column of the channel.

In this section, we present the effect of the control parameters variations on the flow structure and the thermal field. These will be presented as streamlines and isotherms for the following dimensionless geometrical parameters: $D=0.2$, $L=10$, $H=5$.

Values	Dimensional value	Dimensionless value
Diameter	0.2m	1
Lenght	2m	10
Depth	1m	5

4.1 Flow structure and thermal field

In this paragraph, we discuss the Reynolds number effect on the flow structure and thermal filed. We have identified two main areas of the Reynolds number in the range $100 \le \mathrm{Re} \le 700$. A range of low values of $\mathrm{Re}\,(100 \le \mathrm{Re} \le 500)$ in which Nu increases with R; and a second zone of, relatively, high values of $\mathrm{Re}\,(500 \le \mathrm{Re} \le 700)$ wherein Nu decreases when Re increases. This will be discussed in the next paragraph.

Only typical representative figures of the flow structure and corresponding isotherms will be presented in this paper.

For low values of Reynolds, the streamlines are almost parallel to each other and to the walls of the channel, as shown in figure 2 (in the right), for $\mathrm{Re}=300$. The boundary lines laminate the walls except in the lower corners of the channel, wherein a flow separation appears inducing the appearance of a small recirculation zone. So, we get a simple flow structure. The thermal field (left) shows that the heat exchange between the walls and the ventilation jet of fresh air is mainly performed in the vertical column on the right. Indeed, the velocity of ventilation at the inlet is still weak (and therefore low mass flow rate) and favors a limited heat transfer in the vertical air intake column. We note that in the rest of the channel, there is practically no heat exchange between the active walls and the inside air. Increasing Re, a flow stagnation zone appears at the corners, figures 3 and 4, for $\mathrm{Re}=400$ and 500, respectively. The one on the right corner is stronger than the left.

This may be due to the reversal of the flow direction (opposite to gravity in the right corner and the contrary, in the left corner). Note also that the two modes of natural convection and forced convection operate in the opposite direction (right column) and in the same direction (left). Narrowing zones are increasing progressively, as Re increases, until appearance of the recirculation cells at the two corners, figure 5, $\mathrm{Re}=600$. The structure of the flow becomes relatively complex.

Thermal fields in these various figures show that, in general, air is not fully heated for not exceeding $\mathrm{Re}=400$. Indeed, in figures 2 and 3, the air still fresh represented by the green and yellow colors, can not exceed half of the channel. Beyond the length $\mathrm{L}/2$ in the direction of flow, the air has become fairly hot (orange or red) which destroyed the heat transfer between the hot wall and the fluid. For $\mathrm{Re}=500$, yellow tongue arrives until mid height of the right column. This further improves the heat exchange between the walls and air. Taking $\mathrm{Re}=600$, the fluid flows with a relatively high speed and thus the residence time in the channel is short enough that it does not allow a good heat exchange. This explains the existence of the yellow zone reaches the outlet of the channel.

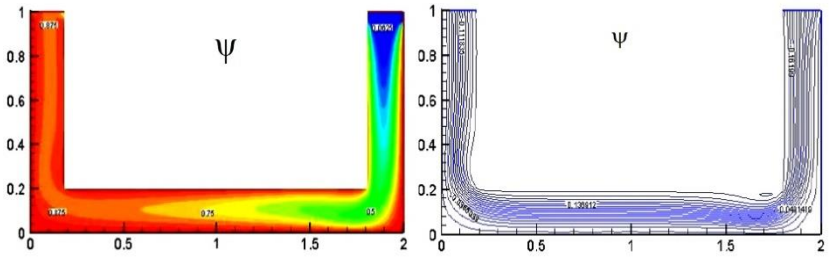

Fig. 2: Isotherms and Streamlines for $\mathrm{Re}=300$, $\mathrm{Ra}=10^5$

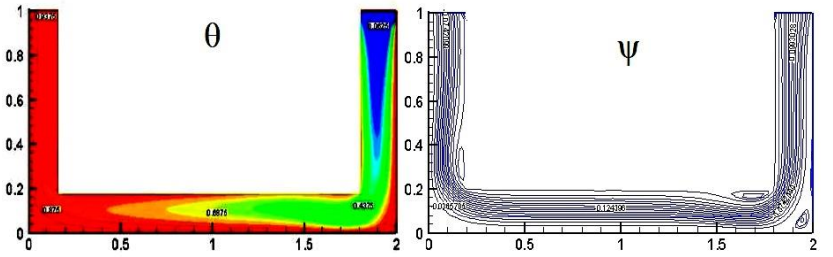

Fig. 3: Isotherms and Streamlines for $\mathrm{Re}=400$, $\mathrm{Ra}=10^5$

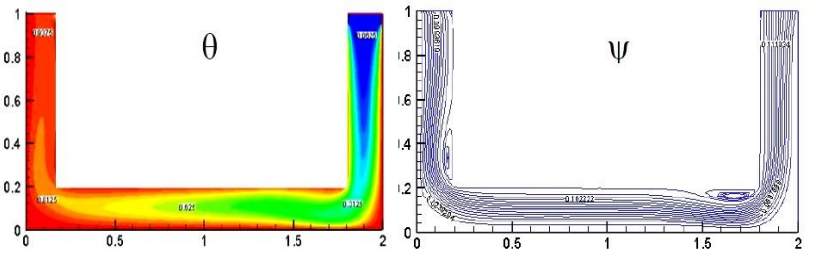

Fig. 4: Isotherms and Streamlines for $\mathrm{Re}=500$, $\mathrm{Ra}=10^5$

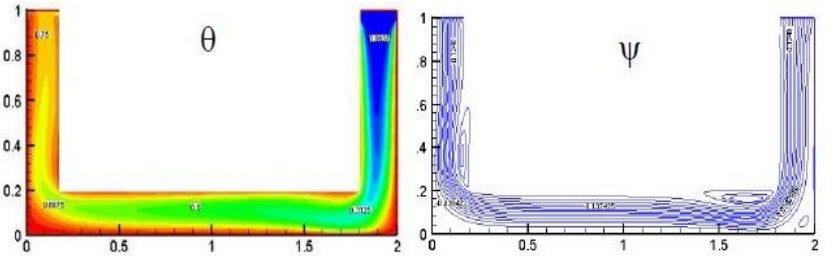

Fig. 5: Isotherms and Streamlines for $\mathrm{Re}=600$, $\mathrm{Ra}=10^5$

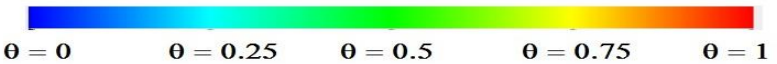

4.2 Quantitative study

In this section, we present the effect of the Reynolds number variation on the temperature and the velocity at the outlet of the channel for $\mathrm{Ra}=10^5$, and the global Nusselt number variation with Re.

The knowledge of the velocity profiles and temperature at the outlet of the channel informs us about the amount of energy won by the air from its entry to its exit from the channel. It is therefore important to examine the evolution of these two variables. In figures 6 and 7, we present the profiles $\theta(x)$ and $V(x)$, respectively for $\mathrm{Re}=100$ and $\mathrm{Re}=700$. We also find that along the greater part of the discharge opening, the air exits at a temperature near than the walls. The velocity, for its part, does not exceed the value of 1.2 (dimensionless value). When Re increases, the thermal profile loses slightly its symmetrical property. We note in Figure 7 that the air lives the channel more cold compared to the previous case. The velocity profile becomes symmetrical with an important maximum value.

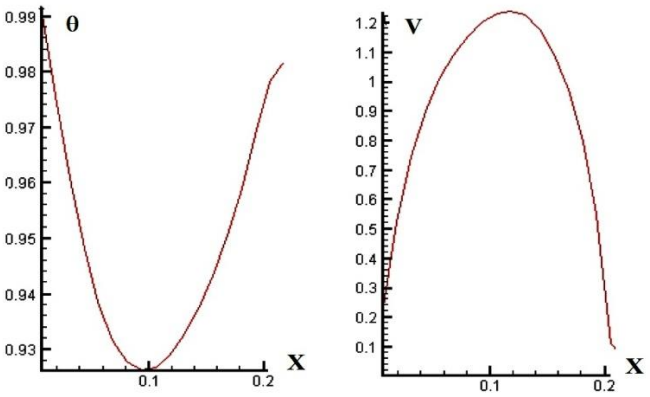

Fig. 6: Temperature and velocity variation with X at the channel outlet, Re=100

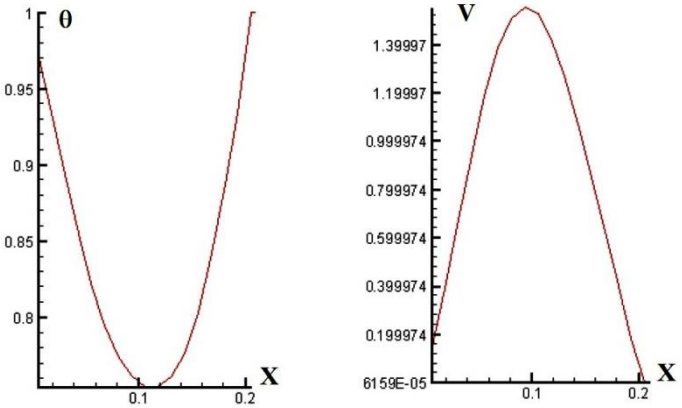

Fig. 7: Temperature and velocity variation with X at the channel outlet, Re=700

4.3 Heat transfer

The heat transfer between the walls of the channel and the fresh air is evaluated in terms of global Nusselt number Nu .

Its variation according to the Reynolds number is presented in figure 8.

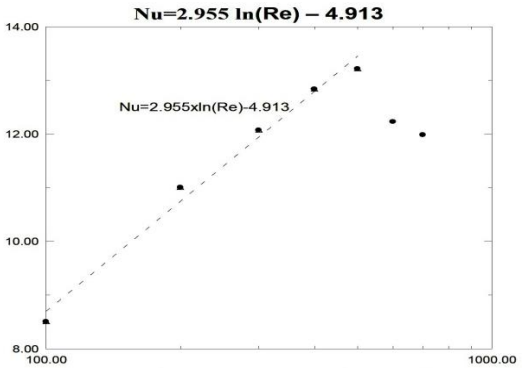

Fig. 8: Nusselt number variation with Reynolds number

We note that Nusselt number increases with Re number until the value of $Re = 500$ when it reaches its maximum value $Nu_{max} = 13.21$ and then decreases slightly for the higher values of Re.

We have correlated Nusselt number with Re number int the range of Re as: $100 \leq Re \leq 500$. We have correlated the variation of Nusselt number with Re number as shown below.

4. CONCLUSION

We conducted a numerical investigation of mixed convection flows in a U-shaped channel with heated walls and submitted to forced fresh air jet. This configuration represents a Canadian well (air-ground heat exchanger) for passive air heating in winter.

We presented in this paper, the first results obtained in terms of the flow structure and heat transfer. These results show that:

- At low values of the Reynolds number, the heat exchange is limited to the right vertical column of the channel.

- The major part of the channel is almost isothermal.

- When Re increases, there is an important improvement of heat exchange along all the walls of the channel.

- When Re further increases, recirculation cells appear and cause a throttling of the flow on the corners of the channel.

- The Nusselt number presents a maximum around the $Re = 500$ value.

NOMENCLATURE

d, Channel diameter, m	D, Dimensionless channel diameter
g, Gravity acceleration, m/s^2	h, Depth of the channel, m
H, Dimensionless depth of the channel	L, Dimensionless channel length, m
l, Length of the channel, m	P, Driving pressure, Pa
Nu, Global Nusselt number	Pr, Prandtl number, $Pr = \nu / \alpha$
Ra, Rayleigh number, $Ra = g.\beta.\Delta T.d^3 / (\alpha.\nu)$	β, Volumetric coefficient of thermal expansion
Re, Reynolds number, $Re = V_{in}.d/\nu$	α, Thermal Diffusivity, m^2/s
T, Temperature, °C	ν, Kinematic viscosity of fluid, m/s
θ, Dimensionless Temperature, $\theta = (T - T_C) / (T_H - T_C)$	ΔT, Temperature difference, $(= T_H - T_C)$
Ψ, Dimensionless stream function, $(= \nu / \alpha)$	φ, Stream function, m^2/s
	m, average, out, outlet, in, inlet
	C, Cold, H, Hot, max, Maximum

REFERENCES

[1] P. Hollumer, '*Utilisation des Echangeurs Air/Sol pour le Chauffage et le Rafraîchissement des Bâtiments*', Thèse de Doctorat, Université de Genève, 2002.

[2] S. Thiers, '*Etude Géothermique du Sud de l'Algérie*', Mémoire de Magister, Université M'Hamed Bouguerra, Boumerdes, 2006.

[3] K. Dehina et A.M. Mokhtari, '*Simulation Numérique d'un Echangeur Air-Sol-Eau à Co-Courant*', XXX^{èmes} Rencontres AUGC-IBPSA, Chambéry, Savoie, 6-8 Juin, 2012.

[4] N. Nali, S. Kooli et A. Ferhat, '*Optimisation Analytique et Validation Expérimentale d'un Echangeur Enterré*', Revue des Energies Renouvelables, Vol. 13, N°3, pp. 525 – 535, 2010.

[5] B. Mebarki, B. Draoui, S. Abdessamad, A. Keboucha, S. Drici et A. Sahli, '*Etude d'un Système de Climatisation Intégrant un Puits Canadien dans les Zones Arides, Cas de Béchar*', Revue des Energies Renouvelables, Vol. 15, N°3, pp. 465 – 478, 2012.

[6] G. de Wahl Davis and I.P. Jones, '*Natural Convection in a Square Cavity: A Comparison Exercise*', International Journal for Numerical Methods in Fluids, Vol. 3, pp. 227 – 248, 1983.

[7] M. Kriraa, M. El Alami, M. Najam and E. Semma, '*Improving the Efficiency of Wind Power System by Using Natural Convection Flows*', Fluid Dynamics & Materials Processing, Vol. 7, N°2, pp. 125 - 140, 2011.

[8] N. Sabour, M. Faraji, M. Najam, M. Kriraa and M. El Alami, '*Natural Convection Flows in a Vertical Semi Convergent Channel with an Obstacle*', International Journal of Engineering and Manufacturing Science, Vol. 2, N°2, pp. 71 – 85, 2012.

[9] J.P. Van Doormaal and G.D. Raithby, '*Enhancements of the SIMPLE Method for Predicting Incompressible Fluid Flows*', Numerical Heat Transfer, Vol. 7, N°2, pp. 147 – 163, 1984.

[10] G. de Vahl Davis, '*Natural Convection of Air in a Square Cavity: A Bench Mark Numerical Solution*', International Journal for Numerical Method in Fluid, Vol. 3, N°3, pp. 249 – 264, 1983.

[11] P. Le Queré and T. Alziary de Roquefort, '*Computation of Natural Convection in 2-D Cavities with Chebyshev Polynomials*', Journal of Computational Physics, Vol. 57, N°2, pp. 210 – 228, 1985.

[12] D. Kalache, F. Penot and F. Le Quéré, '*Numerical Investigation of the Validity of the Two-Dimensional Assumption in the Computation of Natural Convection within a Trapezoidal Cavity*', Numeric Methods In Laminar And Turbulent Flow, 4th International Conference, Swansea, UK, pp. 829 – 840, 1985.

[13] G. Desrayaud and A. Fichera, '*Laminar Natural Convection in a Vertical Isothermal Channel with Symmetric Surface Mounted Rectangular Ribs*', International Journal of Heat and Fluid Flow, Vol. 23, pp. 519 – 529, 2002.